J. Phys. Chem. A **1997,** *101,* 5805−5812

Stationary Points on the Ground-State Potential Energy Surface of Dimethyldiazene. Isomerization and Decomposition in Competition

Imrich Vrábel,* Stanislav Biskupič, and Andrej Staško

Department of Physical Chemistry, Slovak University of Technology, Radlinského 9,
SK-81237 Bratislava, Slovak Republic

Received: February 26, 1997; In Final Form: May 6, 1997[⊗]

The singlet ground-state potential energy surface as related to the thermal unimolecular mechanisms of dimethyldiazene was investigated, in order to obtain activation energies for *trans*−*cis* isomerization, as well as for the isomerization leading to 1,1-dimethyldiazene and for the simple C−N bond cleavage in the formation of $CH_3N_2^•$ and $CH_3^•$ radicals. We used approximate density functional theory (DFT) with B3LYP potential to locate minimum energies and transition-state structures, as well as to determine harmonic vibrational frequencies and resulting zero-point vibrational energies. To obtain more reliable results, some structures were reoptimized by the multiconfiguration SCF wave function. The energetics were determined using quadratic configuration interaction singles and doubles (QCISD), perturbation theory with UHF and CAS reference wave functions (MP2-MP4 and CASPT2), and the configuration interaction wave function, which includes single and double excitations from the selected set of reference configurations constructed with the CASSCF molecular orbitals (MR-CISD). In contrast to previous theoretical studies, our results show that the *trans*−*cis* isomerization of 1,2-dimethyldiazene, which proceeds by rotation around the N═N bond, or semilinearization, requires an activation energy near to that of its decomposition. It was also confirmed that isomerization to 1,1-dimethyldiazene is less favored than the *cis*−*trans* isomerization. The following barrier heights have been estimated: 229 kJ/mol for decomposition, 207 kJ/mol for isomerization by rotation, 227 kJ/mol for isomerization by semilinearization, and 424 kJ/mol for rearrangement to 1,1-dimethyldiazene. Calculation of RRKM rate coefficients showed that in the temperature range from 450 to 600 K the *trans*−*cis* isomerization and a direct decomposition proceed in competition. However the more stable *trans*-1,2-dimethyldiazene preferentially decomposes directly, as a consequence of the fast reverse *cis*−*trans* isomerization rate. At the temperatures above 600 K a direct decomposition increasingly predominates over isomerization.

Introduction

Azo compounds, characterized by the −N═N− functional group, have attracted considerable attention in the literature.[1] Interest in this topic extends to almost every branch of chemistry. There has been considerable interest in azo compounds as powerful and selective reducing agents,[2] as a source of free radicals,[3] for the study of thermal[4] and photochemical[5] fragmentation, and for a model study of unimolecular reaction theory.[6] Furthermore, theoretical chemists have been interested in the mechanisms of decomposition[7,8] and isomerization[9,10] of diazenes. However, despite the activity in this area, the available experimental thermochemical, and structural data for azo compounds are rather limited, by comparison with their isoelectronic alkene analogues. Such information is desirable in order to have a better understanding of azo chemistry.

An alternative source of such data comes from theoretical studies. Numerous calculations on 1,2-diazene (N_2H_2) have been concerned with the mechanisms for interconversion among its three isomers,[11,12] in particular the hydrogen shifts that occur during the *trans*−*cis* and *trans* → 1,1-diazene rearrangements. Three mechanisms of the thermal reversion of *trans*-1,2-diazene to the *cis* isomer were envisioned: rotation around the N═N double bond, inversion through one nitrogen (semilinearization) and dissociation to diazenyl and hydrogen radicals, and recombination. In 1973 Bair and Svenson[13] suggested that azoalkanes, as a consequence of symmetry-forbidden orbital crossing, do not follow the rotational pathway. In a subsequent paper,[14] Winter and Pitzer (1984) confirmed this suggestion. This conclusion was based on the rather rough calculation of the rotation barrier using a two-configuration SCF wave function. Since then, a hypothesized transition state corresponding to inversion at one nitrogen atom (semilinearization) has been preferred over internal rotation around the N═N bond. It was shown in recent papers[15,16] that the *trans*−*cis* semilinearization barrier is about 220 kJ/mol, which is 85 kJ/mol lower than the N−H bond dissociation energy in *trans*-1,2-diazene. For isomerization of *trans*-1,2-diazene to 1,1-diazene a barrier height of 297 kJ/mol was found, which indicates that dissociation−recombination and isomerization pathways are likely to be competitive.

While there have been several detailed theoretical investigations of the parent diazene molecule, calculations on the larger and more stable azo compounds have been rare. Because the chemistry of diazene is significantly different from that of azoalkanes, calculations on a molecule like 1,2-dimethyldiazene should provide a more faithful model for understanding the properties of azo compounds of moderate complexity.

Only two *ab initio* computations have been reported so far for the 1,2-dimethyldiazene isomerization process, and neither of these has gone beyond the SCF level to include the effect of electron correlation. Epstein and Steel[17] established by the partial retention of diatomic differential overlap (PRDDO) method, in a minimal basis set, that for *trans*-1,2-dimethyldiazene the ground-state rotational barrier is 305 kJ/mol, which is about 85 kJ/mol higher than the barrier for semilinearization. These calculations were in good agreement with the RHF/STO-3G results of Howell and Kirschenbaum.[18]

---

* Corresponding author: vrabel@theochem.chtf.stuba.sk.

[⊗] Abstract published in *Advance ACS Abstracts,* July 15, 1997.

S1089-5639(97)00702-0 CCC: $14.00

Only a single work (Schaefer *et al.*[7]) involving calculation of 1,2-dimethyldiazene decomposition correlation effects through the CC-SD(T) method has been published. They established that the more stable *trans*-1,2-dimethyldiazene isomer lies 41 kJ/mol lower than the *cis* isomer. These calculations also found a barrier to dissociation of 196 kJ/mol after inclusion of zero-point energy corrections. In this paper we report a series of calculations that have been undertaken in an attempt to explain several aspects of the thermal behavior of acyclic azoalkanes. We focus here primarily on the mechanisms of *trans*−*cis* isomerization of 1,2-dimethyldiazene and on its rearrangement to 1,1-dimethyldiazene.

Theoretical Approach

All considered structures have been optimized by an energy gradient method at the B3LYP level in which the three-parameter Becke exchange functional[19] was added to the LYP[20] correlation potential. In these electronic structure calculations we employed a restricted version for closed-shell systems and an unrestricted version for open-shells and saddle points. At the geometry optimizations a tight convergence criterion for the gradient was applied (0.000 015 hartree/Å), as some structures were very close in energy. Normal coordinate analysis has been carried out at the same level in order to identify the optimized stationary points and to calculate zero-point energies, which were obtained by scaling the B3LYP frequencies by 0.95. This scaling factor resulted from the fitting of the calculated vibrational frequencies to the experimental ones. The energetics of the structures were improved by using a single-point Møller−Plesset perturbation theory (MP2-MP4)[21] and also by the quadratic CI (QCISD)[22] method. In the unrestricted versions the annihilation of the spin contaminants was performed by the Schlegel algorithm.[23] The stability of the UHF wave function was tested[24] using single-excitation configuration interaction (stability test available in G92/DFT). The UHF wave functions were found to be stable with respect to perturbation from the excited configurations with the exception of the rotational transition state. It is well-known that the isomerization of 1,2-dimethyldiazene by rotation about the N═N bond is symmetry-forbidden, and therefore several configurations become near-degenerate along the reaction path. The CASSCF wave function has been used for the description of the near-degeneracy correlation effect; this function is formed by including all possible singlet-spin configurations distributing a number *n* of active electrons among a number *m* of active molecular orbitals (*n*-in-*m*). At this level of theory the rotational transition state was optimized. Since the comparison of barrier heights for different reaction channels is appropriate only when using identical methods, we performed a CASSCF electronic structure calculation on the *trans*-1,2-dimethyldiazene and the semilinear transition-state structure too. The dynamical correlation effect was calculated by means of second-order perturbation theory from the CASSCF reference wave function (CASPT2)[25] and by CI wave functions including all single and double excitations from a selected set of MCSCF reference configurations (MR-CISD).

Two basis sets were used in this study. The first, DZP, reported by Huzinaga and Dunning,[26] is the standard double-ζ basis set augmented by a single set of polarization functions on each of the atoms. This basis set is designated as C,N (9s5p1d/4s2p1d), H (4s1p/2s1p). Orbital exponents for the polarization functions are $\alpha_d(C) = 0.75$, $\alpha_d(N) = 0.8$, and $\alpha_p(H) = 0.75$. The second basis set, denoted TZ2P,[27] is the Huzinaga−Dunning triple-ζ plus double polarization basis set designated as C,N (10s6p2d/5s3p2d) and H (5s2p1d/3s2p1d). Pure sets of d functions (i.e. five d functions) were used in this study. The MR-CI calculations described above include about 370 000 configurations for each reference configuration in the DZP basis set.

All electronic structure calculations were carried out by GAUSSIAN 92/DFT[28] and MOLCAS 3[29] program packages.

Geometries

The selected geometrical parameters for 1,2-dimethyldiazene and relevant stationary points are given in Figure 1. The experimental geometries[30,31] have been established for *trans*-**I** and *cis*-1,2-dimethyldiazene-**II** only, as the experimental values for the other structures are not available. The calculated geometries (**I**, **II**) are in reasonable agreement with experiment, the deviations in bond lengths and bond angles being 0.02 Å and 2°, respectively. On the basis of these results, a similar accuracy can be expected for the calculated saddle point geometries.

The performance of the HF and CISD methods with various basis sets has been intensively examined in a previous study by Schaefer *et al.*[7] Our B3LYP/DZP calculations compare well with Schaefer's. They used a basis set of the same quality as ours; however, in their paper an unexpected distortion from C_{2v} symmetry was observed for structure **II**, which was not evident in our calculations.

It is noteworthy that the N−N bond length in 1,1-dimethyldiazene (structure **III**) is shorter by 0.03 Å relative to the N−N bond distances in structures **I** and **II**. This shortening of the N−N bond length is also reflected in the intermediate bond order. The natural bond orbital analysis of the QCISD wave function assigns 4.748 electrons on the N−N bonding orbitals, implying a bond order of 2.374. Natural bond orbital analysis also shows 2.876 lone pair electrons on the nitrene nitrogen. The shortening of the bond length and increasing of the bond order is probably attributed to π donation from the CH_3-N-CH_3 group into a vacant π orbital on the nitrene nitrogen.

The calculated geometries of radical products (structures **VII** and **VIII**) were compared with the theoretical predictions published by Hu and Schaefer.[32] Our optimized N−N and C−N bond lengths are longer by 0.01 and 0.02 Å, respectively, than the bond lengths obtained at the TZ2P+f CISD level. The remaining parameters are accurately reproduced.

We shall now turn to a discussion of the transition-state geometries. In the rotational transition state **IV** the reacting N−N bond is stretched and is virtually broken. The elongation of the N−N bond by 0.04 Å and shortening of the C−N bond by 0.01 Å indicated that the electrons from the partially broken N−N π-bonding orbital are redistributed on the C−N σ orbitals. The natural bond orbital analysis verifies this suggestion, because the decreasing of bond order from 1.646 to 1.524 was found for the N−N bond. The C−N−N−C torsional angle of the transition structure was predicted to be about 89.9°. Reoptimization of the geometrical parameters by the 4-in-4 CASSCF method does not change the structural parameters of the transition state significantly.

Somewhat surprisingly, the structure of the semilinear transition state **V** was found to be slightly distorted from C_s symmetry. For the C−N−N−C torsional angle the value of 9.5° was found at a bond angle 178.6°. The reacting C−N bond for the inversed methyl group is only slightly stretched, but the opposite C−N bond length is shortened by 0.08 Å relative to the **I**.

For the transition structure **VI** (between species **I** and **III**) C_1 symmetry was found. To investigate this further, we

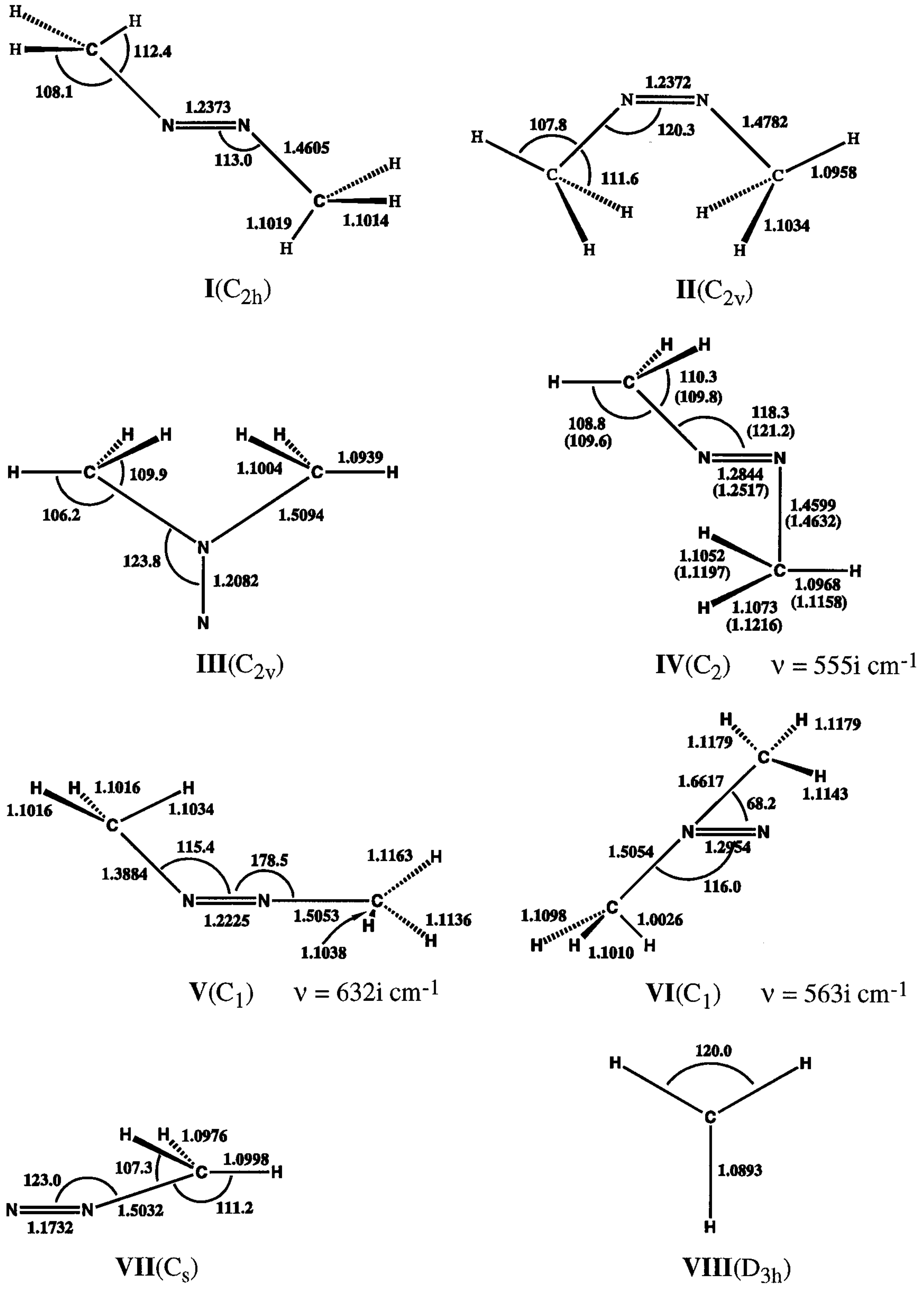

Figure 1. Investigated structures **I**−**VIII** with some selected B3LYP/DZP optimized geometrical parameters. Bond lengths are given in angstroms and bond angles in degrees. For structure **IV** the geometrical parameters in parentheses are calculated at the 4-in-4 CASSCF level.

calculated the wave function of **VI** at the average C_s geometry. This resulted in a symmetry-broken wave function with an exception, when symmetry was explicitly enforced during the 4-in-4 CASSCF optimization. Also an extended calculation with two additional orbitals in the active space and two additional active electrons (6-in-6 CASSCF) displayed the same behavior. We note that Pople *et al.*[15] observed the same behavior of the transition state for isomerization of *trans*-1,2-diazene to 1,1-diazene.

Energetics of Reactants and Products

The potential energy surface associated with structure **I** is relatively complex, because of the existence of three isomers (**I**, **II**, and **III**) and four exit channels (Scheme 1). Regarding the relative energies, we first examine the energies of the stable isomers for which some theoretical predictions are available. The relative energies, including the corrections for the difference in the zero-point vibrational energies at the B3LYP/DZP level, are given in Table 3. The energy difference between structures

SCHEME 1

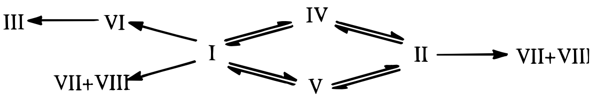

TABLE 1: Calculated Total[a] and Zero-Point[b] Energies (in hartrees) for Dimethyldiazenes (I−VI) and Their Decomposition Products (VII, VIII)

structure	B3LYP	MP2[c]	QCISD	ZPE
I	−189.256 094	−188.675 536	−188.718 735	0.083 719
II	−189.239 694	−188.658 648	−188.701 976	0.083 047
III	−189.217 919	−188.630 266	−188.678 643	0.083 349
IV	−189.146 033	−188.557 296	−188.599 185[d] −188.585 200	0.080 129
V	−189.176 174	−188.584 107	−188.628 286	0.080 823
VI	−189.109 367	−188.500 920	−188.552 752	0.079 628
VII	−149.333 787	−148.893 211	−148.924 845	0.043 269
VIII	−39.834 483	−39.689 165	−39.709 497	0.029 366

[a] Based on B3LYP/DZP optimized geometries. [b] Zero-point energies from B3LYP/DZP and scaled by 0.95. [c] For open-shell species a projected wave function was used (PMP2). [d] The total energies were calculated from RHF wave functions for $(8b)^2(9a)^0$ and $(8b)^0(9a)^2$ configurations; see text.

TABLE 2: Calculated Total Energies (in hartrees) of Structures I, VII, and VIII at Various Levels of Perturbation Theory[a]

basis	method	**I**	**VII**	**VIII**
DZP	UHF	−188.055 077	−148.454 712	−39.554 784
	MP2	−188.675 536	−148.893 211	−39.689 165
	MP3	−188.707 209	−148.912 309	−39.706 857
	MP4	−188.715 657	−148.916 644	−39.708 493
TZ2P	UHF	−188.103 018	−148.488 075	−39.568 029
	MP2	−188.804 187	−148.992 151	−39.712 435
	MP3	−188.828 190	−149.006 258	−39.729 931
	MP4	−188.845 583	−149.019 397	−39.732 278
TZ2P+f	UHF	−188.111 586	−148.493 449	−39.568 337
	MP2	−188.863 240	−149.033 022	−39.721 512

[a] For open-shell species a projected wave function was used.

TABLE 3: Calculated Relative Energies[a,b] (in kJ/mol) for Structures I−VIII

structure	B3LYP	MP2	QCISD
I	0.00	0.00	0.00
II	41.18	42.46	42.12
III	99.04	117.65	104.07
IV	204.03	225.47	228.90[c] 237.67
V	201.85	232.02	229.45
VI	373.84	446.95	424.31
VII+VIII	206.15	215.09	194.10

[a] The relative energies are corrected for zero-point vibrational energies. [b] Based on the total energies in Table 1. [c] Calculated relative energies for different electron configurations; see Table 1.

I and **II** is of particular interest, as they represent the simplest *cis*−*trans* azoalkane pair. For the sake of comparison, the energy difference between the prototypical *cis*−*trans* 1,2-diazene pair is 20.9 kJ/mol, calculated at the G2 level of theory.[33] Table 3 shows that the best estimation for the *cis*−*trans* energy gap of 42.1 kJ/mol is quite comparable to the calculated value of 40.9 kJ/mol determined by Schaefer *et al.*[7]

Structure **III** has not yet been isolated or detected by spectroscopic methods, but 1,1-dialkyl-diazenes are assumed as intermediates in many chemical reactions.[34] These presumed intermediates show behaviors suggesting that the reacting species are the singlet in contrast to other nitrenes, e.g. alkyl, aryl, and cyano nitrenes, which have the triplet ground state.[35] Our 2-in-2 CASSCF/DZP calculations have shown that the $^3A_2$ triplet state lies 52.1 kJ/mol above the $^1A_1$ singlet ground state. The energy gap between **I** and **III** in their ground state is 104 kJ/mol, which indicates that the 1,1-dimethyldiazene is less stable than structure **II**.

TABLE 4: Calculated Bond Dissociation Energies D_e(C−N)[a] (in kJ/mol) for the Decomposition of *trans*-$CH_3-N{=}N-CH_3 \rightarrow CH_3N_2^\bullet + CH_3^\bullet$

	DZP	TZ2P	TZ2P+f
UHF	119.48	122.98	130.54
MP2	244.20	261.08	284.95
MP3	230.79	241.19	
MP4	237.28	246.16	

[a] Based on the total energies in Table 2.

Energetics of the C−N Bond Fragmentation Reactions

A precise experimental D_0(C−N) bond dissociation energy for structure **I** has not yet been determined; the values published so far are in the range from 210 to 232 kJ/mol. The highest value was reported by Forst and Rice.[36] They assumed that the decomposition proceeds via a chain mechanism, and they inhibited the reaction by NO in order to obtained intrinsic bond dissociation energies. Hu *et al.*[7] investigated this barrier height theoretically via the CC-SD(T)/TZ2P technique and predicted a value of 194 kJ/mol. In Table 3 and 4 the D_e(C−N) bond dissociation energies at several levels are summarized, as determined from the total energies listed in Tables 1 and 2 considering B3LYP/DZP structures. The spin contaminations in the UHF reference wave functions for open-shell species (**VII**, **VIII**) are small: the expected values of S^2 differ by less than 0.12 in units of $\hbar^2$ from the correct value of 0.75. From data in Table 3 it is apparent that with each basis set the MP2 perturbation correction steps over the exact correlations, which are not fully damped even at fourth order. Somewhat unexpectedly the MP3−MP4 shift yields only a 4−8 kJ/mol increase in D_e(C−N).

Extensive *ab initio* studies[37] on diatomic molecules have clearly shown that flexible basis sets and, in particular, high angular momentum functions are indispensable for recovering the correlation contribution to bond energies. For example, at the MP4(SDTQ) level, an increase of 38.0 kJ/mol in the dissociation energy of N_2 is observed upon addition of f functions to the 6-311G(d,p) basis set. Similarly, transition from DZP to TZ2P increases D_e(C−N) by 9 kJ/mol at the PMP4 level, giving an overall value of 246 kJ/mol. Surprisingly, the inclusion of an extra set of higher order angular momenta to the TZ2P basis set (d-type functions on H, $\alpha_d(H) = 1.0$; and f-type functions on C and N atoms, $\alpha_f(C) = 0.8$, $\alpha_f(N) = 1.0$) increased the barrier by 24 kJ/mol at the PMP2 level. Basis set deficiencies of 24 kJ/mol or more are likely to be present in this prediction, consistent with the TZ2P and TZ2P+f PMP2 energies in Table 4, but the resulting shift toward larger dissociation energies will be balanced by the effects of spin contamination, basis set superposition error, and higher order perturbation energy contributions. On the basis of the previous discussions, the predicted bond dissociation energy D_e(C−N) is 270 kJ/mol.

The other way to correct the calculated bond dissociation energies comes from Gordon and Truhlar.[38] They found that the dissociation energy of the simple C−N bond is underestimated by 20 kJ/mol with respect to the experiment at the MP4/6−311G** level. Referring to the discussion above and the MP4/6−311G** C−N bond dissociation error, our C−N bond dissociation energy calculated with a similar TZ2P basis set might be expected to be 266 kJ/mol. In contrast to this, the

QCISD/DZP bond dissociation energy is merely 221 kJ/mol, although after the basis set correction it may be 245 kJ/mol. The D_e(C−N) values predicted by various methods differ up to 25 kJ/mol. Our final proposal for D_e(C−N) is 257 kJ/mol, to which error bars of ca. 12 kJ/mol are to be associated. After the corrections to the zero-point energies, we predict a D_0(C−N) of 229 kJ/mol, which favors a value near the upper limit of the experimental range.

The rates and activation parameters of 1,1-dimethyldiazene thermal reactions are unknown. Previous theoretical studies suggest that the C−N bond strength of structure **III** is substantially lower than that of isomer **I**. The homolytic decomposition of **III** was calculated to be endothermic by 98 kJ/mol. The estimation was based on a large basis set GVB-CI calculation of the N−H bond energy of 1,1-diazene and corrected for the difference (77 kJ/mol) between the N−H and N−CH_3 bond strengths. Our QCISD/DZP result of 78 kJ/mol, corrected to zero-point energies, lies 20 kJ/mol below previous theoretical results.

Energetics of Isomerization Reactions

In most experimental conditions, the isomerization of azoalkanes is energetically accessible. It is therefore of interest to evaluate their barrier heights and to compare these barriers with the other channels, since such isomerizations may complicate and also modify the dynamics of the decomposition reactions. Unfortunately, the barriers of the 1,2-dimethyldiazene isomerization reaction were not experimentally established; however the experimental *cis*−*trans* activation energy of 184 kJ/mol for 1,2-diisopropyldiazene has been proposed by Steel *et al.*[39]

The barrier height of 424 kJ/mol for rearrangement **I** → **III**, calculated at the QCISD/DZP level, precludes the possibility of dissociation of **I** via structure **III**. The *trans*−*cis* isomerization process was investigated from similar considerations. As was shown, the rotational transition state of the *cis*−*trans* isomerization in the ground electronic state cannot be represented by a single determinant wave function, because it results from the crossing of two states. A rotation around the N−N axis of **I** or **II** lowers the symmetry of the transition state to C_2. This group will have two configurations:

$^1A_1$: $[...6b^2 7a^2 8a^2 7b^2 8b^2]$

$^1A_1$: $[...6b^2 7a^2 8a^2 7b^2 9a^2]$

which will be nearly degenerate. It is evident that these electron configurations cannot be represented exactly by a single UHF wave function and that MCSCF calculations would be necessary. One can, however, obtain a rough estimate of the transition-state energy by QCISD calculations based on either the $(8b)^2(9a)^0$ or the $(9a)^2(8b)^0$ RHF wave function at geometry obtained by the 4-in-4 CASSCF method. The fact that two barriers, 229 and 238 kJ/mol (Table 3), respectively, are close to each other implies that the present method was able to take quite reasonable care of the near-degeneracy and dynamical electron correlations.

The more exact energy barriers for the *cis*−*trans* isomerization channels were determined by multireference single- and double-excitation CI calculations using 6-in-6 CASSCF orbitals in DZP basis set. A series of CI calculations were performed at each geometry (**I**, **IV**, **V**) beginning with a single reference CI using the dominant configuration in the MCSCF expansion as a reference. Additional reference configurations were added, one by one, based on the magnitude of their coefficient in the MCSCF expansion. Only four reference configurations could be included which results in ∼1.2 million configurations. Table 5 shows the results of these calculations. The quality of the reference description was established as a function of the energies on the sum of squared coefficients for MCSCF expansion. As is shown in Figure 2, the MR-CISD total energy calculated using a DZP basis set is nearly a linear function of the weight of the reference configurations in the MCSCF expansion at all of the geometries. Linear least-squares fits, calculated for each set of energies, yield nearly parallel lines. Vertical energy separations in Figure 2 correspond to a consistent treatment of the electron correlation. A comparison of the energy separation between structures **I** and **V** for a single reference CI calculation yields a nearly vertical line and the energy separation of 239 kJ/mol, which is close to the best energy separation of 235 kJ/mol. An analogous comparison for the energy separation between structures **I** and **IV** gives a difference of 327 kJ/mol and a substantial nonvertical line. The energy separation is overestimated by more than 110 kJ/mol as compared to the best value of 216 kJ/mol. This is a reflection of the fact that a single reference wave function provides a poor description of the rotational transition state. As can be seen from Figure 2, the CI calculation at this transition state, which is based on two reference configurations, provides a treatment roughly equivalent to a CI calculation with four reference configurations.

TABLE 5: Calculated Relative Energies (in kJ/mol) for Structures IV and V at Various Levels

	MR-CISD				CASPT2	
structure	1[a]	2	3	4	DZP	TZ2P
I	0.00	0.00	0.00	0.00	0.00	0.00
IV	327.28	219.00	217.62	216.76	218.24	212.13
V	239.16	239.62	238.33	235.28	237.15	239.84

[a] Number of reference configurations.

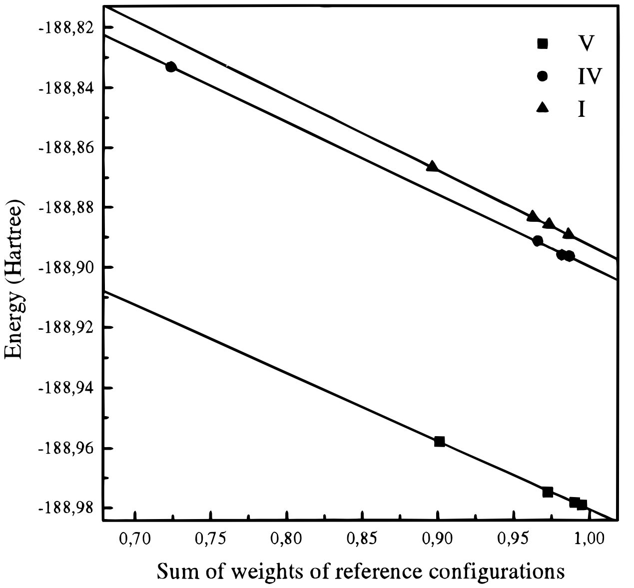

Figure 2. Calculated MR-CISD total energy plotted against the sum of the weights of the reference configurations included in the MCSCF expansion for the structures **I**, **IV**, and **V**.

Our best values for the energy separations were determined as the vertical distance between the lines evaluated at the weight of the reference configurations included in the largest calculation. The basis set dependence of the rotational barrier height was verified by the CASPT2 method with two reference configurations. The relative energies obtained using various basis sets are given in Table 5. From these results it appears that although the influence of the quality of the basis set on the calculated barrier height is marginal, the barrier decreases with

SCHEME 2

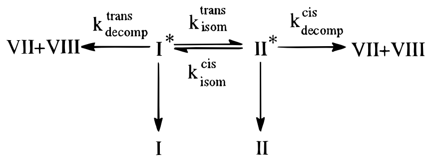

a increasing number of basis functions. This is in accord with the observation that for bond dissociation reactions the high-quality basis set is frequently more important than for molecular rearrangements.[40] On the basis of the calculations presented and experience with other activation energies calculated at a similar level of theory, our best estimation of the activation energy, including the corrections for the difference in the zero-point vibrational energies, for the rotational pathway is 207 kJ/mol and for the semilinearization is 227 kJ/mol. The higher value for semilinearization implies that isomerization of **I** to **II** probably proceeds by a rotational mechanism.

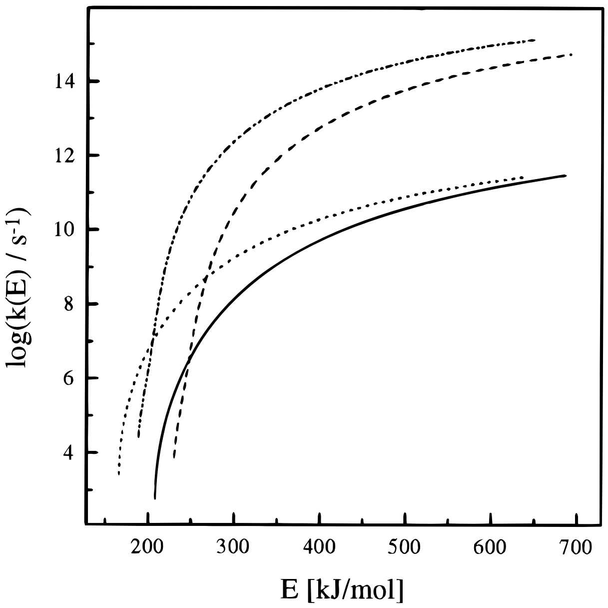

Figure 3. Microcanonical rate coefficients *k*(*E*) as a function of *E* for various reaction pathways: (—) k^{trans}_{isom}, (···), k^{cis}_{isom}, (– – –), k^{trans}_{decomp}, (–··–) k^{cis}_{decomp}.

RRKM Results

The decomposition mechanism of 1,2-dimethyldiazene is extremely complex. The difficulties associated with experimental determination of the mechanisms involved in the dissociation are compounded by the fact that the kinetic parameters are dependent on the temperature. This is because isomerization and dissociation rates are governed not only by transition-state barrier heights but also by the entropy associated with a given rearrangement. In an attempt to obtain more insight into the mechanism of the thermal decomposition of **I**, we have applied the RRKM theory[41] for the calculation of rate constants, to examine the feasibility of various decomposition and isomerization pathways. The decomposition of **I** can be represented in Scheme 2, where **I*** and **I** are the activated and stabilized forms of the isomers. Since the system involves both reversible isomerizations and irreversible decompositions, the relaxation to a thermal distribution of products formed from the excited reactant will occur on a time scale that may be comparable to that for collisional excitation of the reactant. Under this circumstance the calculated rate coefficients will be time-dependent. However, it was shown formally[42] that, even in the early stages of the reaction, the occurrence of the reverse isomerization reaction causes a slowing down in the apparent forward isomerization and decomposition rate coefficients compared to that predicted from the simple largest-eigenvalue result obtained when the reverse reaction is ignored. Zachariah *et al.*,[43] on the basis of the solution of the time-dependent master equation for the system (2-butene) involving isomerization and decomposition, have shown that the reversible isomerization has only a small effect on the decomposition, if the microscopic rate coefficient for the forward reaction is negligible compared to the rate coefficient of the reverse reaction. The relationship between microcanonical rate coefficients $k^{trans}_{isom}(E)$ and $k^{cis}_{isom}(E)$ is dictated by microscopic reversibility:

$$k^{trans}_{isom}(E)\, \rho^{trans}(E) = k^{cis}_{isom}(E - \Delta E)\, \rho^{cis}(E - \Delta E) \qquad (1)$$

where ΔE is the energy difference between species **I** and **II**. It is apparent that the density of states $\rho^{cis}(E - \Delta E)$ will be much smaller than $\rho^{trans}(E)$ at energy E (below 400 kJ/mol) because of the large energy difference $\Delta E = 42.1$ kJ/mol between **I** and **II**. Accordingly, it also appears in the case of microcanonical rate coefficients, as is shown in Figure 3. Under these conditions we can neglect the reversible isomerization and apply a simple irreversible scheme for the formation rate of products, although either at very low pressures or very high temperatures the influence of the relaxation to the equilibrium distribution between *cis* and *trans* isomers on the decomposition rates cannot be unambiguously omitted.

We calculated the high-pressure unimolecular rate constants for individual processes in the rigid rotor, harmonic oscillator approximation using the scaled vibrational frequencies and B3LYP/DZP structures. These RRKM parameters are summarized in Tables 1S-4S (Supporting Information). For decomposition pathways the product-like loose transition states were assumed, in which fragments rotate freely and have the same vibrational frequencies as products. Since the torsional modes below 150 cm^{-1} are likely to be highly anharmonic, these normal mode frequencies were replaced by an appropriate free internal rotation. The reduced moments of inertia for these conjoined torsions were given by $I_{conj} = I_1I_2/(I_1 + I_2)$. The dependence of the rate coefficients on the pressure was established by solution of the master equation by the program UNIMOL.[44] The collision energy transfer probabilities were taken in the standard form of an "exponential down" model[45]

$$P_{ij} = A_{ij} \exp(-(E_j - E_i)/\alpha) \qquad j > i \qquad (2)$$

where α is a positive parameter governing the magnitude of the energy transfer ($\alpha = 500$ cm^{-1}). The values of total collision frequency were calculated using the Lennard-Jones expression,[46] with parameters $\epsilon = 120$ K and $\sigma = 4.1$ Å. The results of these calculations with Ne as the bath gas are presented in Figure 4. It is evident that the shape of the k^{trans}_{decomp} falloff curve strongly depends on the temperature. A similar behavior as described by the *trans* isomer can also be observed for the *cis* isomer. With increasing temperature the dependence on the pressure becomes more and more significant, while on the other hand the *trans*–*cis* isomerization of 1,2-dimethyldiazene is not particularly sensitive to pressure. A behavior similar to that described in the case of the *trans* isomer can also be found for the *cis* isomer. This renders the task of establishing the real decomposition mechanism more difficult. The temperature dependence of the high-pressure rate coefficients is shown in Figure 5. From this it is evident that the large amount of the more stable *trans*-1,2-dimethyldiazene, as expected, is a consequence of the fast reverse isomerization process (with respect

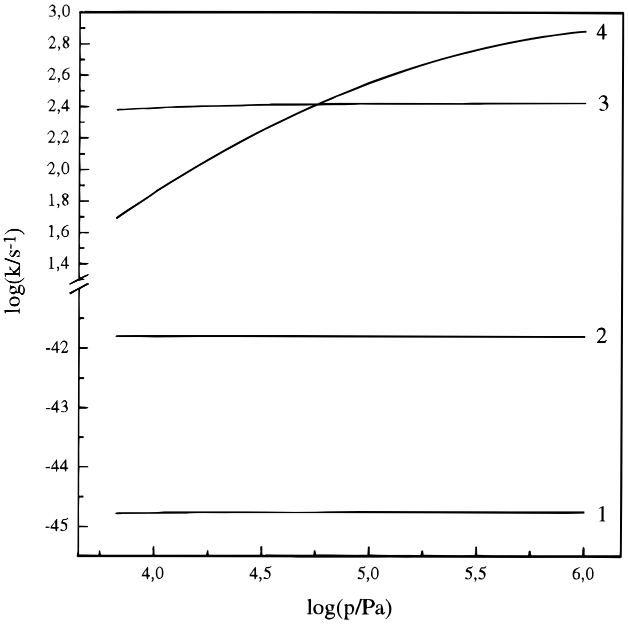

Figure 4. Calculated falloff curves for the decomposition and isomerization pathways at two different temperatures: (1) $k^{\text{trans}}_{\text{decomp}}$ at 200 K, (2) $k^{\text{trans}}_{\text{isom}}$ at 200 K, (3) $k^{\text{trans}}_{\text{isom}}$ at 1000 K, (4) $k^{\text{trans}}_{\text{decomp}}$ at 1000 K.

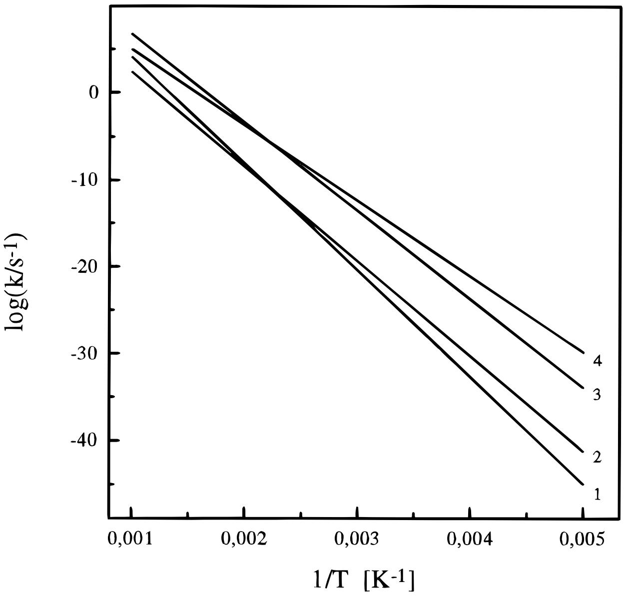

Figure 5. Calculated high-pressure rate coefficients of various unimolecular processes as a function of temperature. (1) $k^{\text{trans}}_{\text{decomp}}$, (2) $k^{\text{trans}}_{\text{isom}}$, (3) $k^{\text{cis}}_{\text{decomp}}$, (4) $k^{\text{cis}}_{\text{isom}}$.

to the decomposition) from structure **II** to structure **I** characteristic for lower temperatures (less than 400 K). At these temperatures the isomerization is the more favorable process and the decomposition of dimethyldiazene, which could proceed via the *cis* isomer, is less probable. At higher temperatures (between 400 and 650 K) the isomerization and decomposition processes are competitive for both species **I** and **II**, independently of pressure. Since *trans* form **I** is more populated, it will primarily decompose via the *trans* isomer, and only a small portion of the products originates from the *cis* isomer. At still higher temperatures (above 650 K) the decomposition pathways predominate over isomerization pathways, and decomposition will also proceed from this point on via the *trans* form. From the data presented it follows that 1,2-dimethyldiazene probably decomposes via the *trans* isomer at the experimentally useful rates. The decomposition via the *cis* isomer becomes significant only at low pressures or low temperatures, when the rate of decomposition is very slow. This is in good agreement with the experimental results of Forst and Rice,[36] and indicates that *trans*−*cis* isomerization is not a necessary precondition for the decomposition of 1,2-dimethyldiazene, contrary to what was proposed earlier by Flamm *et al.*[47] in order to interpret experimental observations.

It should be added that our RRKM calculations represent a relatively reliable approximation. The main uncertainties in the calculated rate coefficients arise from the uncertainties in the threshold energies used in the calculations. Additional imprecision comes from the model used for the decomposition pathways. The rate coefficients with loose transition states should be calculated with more sophisticated models that incorporate the concepts of CVTST (canonical variational transition-state theory). Such improvements to the calculations for the loose transition states would tend to reduce the values of rate coefficients $k^{\text{trans}}_{\text{decomp}}$ and $k^{\text{cis}}_{\text{decomp}}$, and this would favor the direct dissociation of structure **I** at lower temperatures also.

Summary

A reexamination of the dimethyldiazene potential energy surface related to the decomposition and isomerization of *trans*-1,2-dimethyldiazene is presented. Three equilibrium structures and the transition states leading to an isomerization and decomposition of the more stable *trans* isomer were determined. In particular, we have analyzed the reaction pathways for the unimolecular shift of the methyl group in the *trans*-1,2-dimethyldiazene ↔ 1,1-dimethyldiazene rearrangement, for the isomerization by rotation about the N═N bond, and semilinearization leading to the *cis* isomer, and for the various decomposition channels. Our calculations demonstrate the importance of the multireference description of the rotational transition state, which leads to significant decrease of the barrier height. At this level of theory the barrier for rotation is lower than the barrier for semilinearization, suggesting rotation to be the most likely mechanism. Calculations of the rate coefficients for individual reaction pathways have also been carried out in the framework of the RRKM theory. The most important aspect of this contribution is the demonstration that the decomposition channel is the dominant unimolecular pathway for the *trans* isomer at higher temperatures, although the rotational isomerization pathway possesses lower barrier height.

Acknowledgment. The work reported in this paper has been funded by the Slovak Grant Agency, Project No. 1/1395/94.

Supporting Information Available: Tables of RRKM parameters for the decomposition and isomerization of dimethyldiazene (4 pages). Ordering information is given on any current masthead page.

References and Notes

(1) (a) Engel, P. S. *Chem. Rev.* **1980**, *80*, 99. (b) H. Zollinger, *Azo Chemistry*; Verlag Chemie: Weinheim, 1994. (c) Patai, S. *The Chemistry of Functional Groups. Supplement A: The Chemistry of Double-Bonded Functional Groups*; John Wiley and Sons: Chichester, U.K., 1989; Vol. 2, Pt. I.

(2) Miller, C. E. *J. Chem. Educ.* **1965**, *42*, 254.

(3) Pryor, W. A. *Free Radicals*; McGraw-Hill: New York, 1966.

(4) Steel, C.; Trotman-Dickenson, A. F. *J. Chem. Soc.* **1959**, 975.

(5) Burton, K. A.; Weisman, R. B. *J. Am. Chem. Soc.* **1990**, *112*, 1804.

(6) Thomas, T. F.; Sutin, C. I.; Steel, C. *J. Am. Chem. Soc.* **1967**, *89*, 5107.

(7) Schaefer, H. F., III; Hu, C. H. *J. Phys. Chem.* **1995**, *99*, 7507.

(8) (a) Dannenberg, J. J.; Rocklin, D. *J. Org. Chem.* **1982**, *47*, 4529. (b) Dannenberg, J. J. *J. Org. Chem.* **1985**, *50*, 4963.

(9) Mill, T.; Stringham, R. S. *Tetrahedron Lett.* **1969**, 1853.

(10) (a) Schmittel, M.; Rückardt C. *J. Am. Chem. Soc.* **1987**, *109*, 2750. (b) Neuman, R. C., Jr.; Gunderson, H. J. *J. Org. Chem.* **1992**, *57*, 1641.

(11) McKee, M. L. *J. Phys. Chem.* **1993**, *97*, 13608.

(12) Smith, B. J. *J. Phys. Chem.* **1993**, *97*, 10513.

(13) Baird, N. C.; Swenson J. R. *Can. J. Chem.* **1973**, *51*, 3097.

(14) Winter, N. M.; Pitzer, R. M. *J. Chem. Phys.* **1975**, *62*, 1269.

(15) Pople, J. A.; Raghavachari K.; Fisch, M. J; Binkley J. S.; Schleyer, P. R. *J. Am. Chem. Soc.* **1983**, *105*, 6389.

(16) Casewit, C. J.; Goddard, W. A. J. *Am. Chem. Soc.* **1980**, *102*, 4057.

(17) Camp, R. N.; Epstein, I. R.; Steel, C. *J. Am. Chem. Soc.* **1977**, *99*, 2453.

(18) Howell, J. M.; Kirschenbaum L. J. *J. Am. Chem. Soc.* **1976**, *98*, 877.

(19) Becke, A. D. *J. Chem. Phys.* **1993**, *98*, 5648.

(20) Lee, C.; Yang, W.; Parr, R. G. *Phys Rev. B* **1988**, *37*, 785.

(21) (a) Møller, C.; Plesset, M. S. *Phys. Rev.* **1934**, *46*, 618. (b) Krishnan, R.; Fisch, M. J.; Pople, J. A. *J. Chem. Phys.* **1980**, *72*, 4244.

(22) Pople, J. A.; Head-Gordon, M.; Raghvachari, K. *J. Chem. Phys.* **1987**, 5986.

(23) Schlegel, H. B. *J. Phys. Chem.* **1988**, *92*, 3075.

(24) Seeger, S.; Pople J. A. *J. Chem. Phys.* **1977**, *66*, 3045.

(25) Andersson, K.; Malqvist, P. Å.; Roos, B. O. *J. Chem. Phys.* **1992**, *96*, 1218.

(26) (a) Huzinaga, S *J. Chem. Phys.* **1965**, *42*, 1293. (b) Dunning, T. H. *J. Chem. Phys.* **1970**, *53*, 2823.

(27) Dunning, T. H. *J. Chem. Phys.* **1971**, *55*, 716.

(28) Frisch, M. J.; Trucks, G. W.; Schlegel, H. B.; Gill, P. M. W.; Johnson, B. G.; Wong, M. W.; Foresman, J. B.; Robb, M. A.; Head-Gordon, M.; Replogle, E. S.; Comperts, R.; Andres, J. L.; Raghavachari, K.; Binkley, J. S.; Gonzales, C.; Martin, R,T,; Fox, D. J.; Defrees, D. J.; Baker, J.; Stewart, J. J. P; Pople, J. A. *Gaussian 92/DFT*, Revision G; Gaussian, Inc.: Pittsburgh, PA, 1993.

(29) Andersson, K.; Fülscher, M. P.; Lindh, R.; Malqvist P. Å.; Olsen, J.; Roos, B. O.; Sadlej, A. J.; Widmark, P. O. *MOLCAS*, Version 3; University of Lund: Sweden, 1993.

(30) Almenningen, A.; Anfinsen, I. M.; Haaland, A. *Acc. Chem. Scand.* **1970**, *24*, 1230.

(31) Chang, C. H.; Porter, R. F.; Bauer, S. H. *J. Am. Chem. Soc.* **1970**, *92*, 5310.

(32) Hu, C. H.; Schaefer, H. F., III. *J. Chem. Phys.* **1994**, *101*, 1289.

(33) Curtiss, L. A.; Pople, J. A. *J. Chem. Phys.* **1991**, *94*, 7221.

(34) Ioffe, B. V.; Kuznetsov, M. A. *Russ. Chem. Rev. (Eng. Transl.)* **1972**, *41*, 131.

(35) Wasserman, E.; Smolinsky, G.; Yager, W. A. *J. Am. Chem. Soc.* **1964**, *86*, 3166.

(36) Forst, W.; Rice, O. K. *Can. J. Chem.* **1963**, *41*, 562.

(37) Jankowski, K.; Becherer R.; Scharf, P.; Schiffer, H.; Ahlrichs, R. *J. Chem. Phys.* **1985**, *82*, 1413.

(38) Gordon, M. S.; Truhlar, D. G. *J. Am. Chem. Soc.* **1986**, *108*, 5412.

(39) Fogel, L. D.; Rennert, A. M.; Steel, C. *J. Chem. Soc., Chem. Commun.* **1975**, 536.

(40) Mowrey, R. C.; Page, M.; Adams, G. F.; Lengsfield, B. H., III. *J. Chem. Phys.* **1990**, *93*, 1857.

(41) Gilbert, R. G.; Smith, S. C. *Theory of Unimolecular and Recombination Reactions;* Blackwell: Oxford, 1990.

(42) Quack, M. *Ber. Bunsen-Ges. Phys. Chem.* **1984**, *88*, 94.

(43) Bedanov, V. M.; Tsang, W.; Zachariah, M. R. *J. Phys. Chem.* **1995**, *99*, 11452.

(44) Gilbert, R. G. *UNIMOL* program; 1990.

(45) Keck, J. C.; Carrier, G. *J. Chem. Phys.* **1965**, *43*, 2284.

(46) Reid, R. C.; Sherwood, T. K. *The Properties of Gases and Liquids: Their Estimation and Correlation*; McGraw-Hill: New York, 1958.

(47) (a) Seeman, J. I. *Chem. Rev.* **1983**, *83*, 84. (b) Flamm, M.; Beckhaus, H. D.; Rückardt, C. *Tetrahedron Lett.* **1982**, 1805.